BULLETIN OF THE POLISH ACADEMY OF SCIENCES
TECHNICAL SCIENCES, Vol. 68, No. 4, 2020
DOI: 10.24425/bpasts.2020.134171

Control system and measurements of coil actuators parameters for magnetomotive micropump concept

Ł. KOLIMAS[1], K. BIEŃKOWSKI[2], S. ŁAPCZYŃSKI[1], M. SZULBORSKI[1*], Ł. KOZAREK[3], and K. BIREK[3]

[1] Institute of Electrical Power Engineering, Warsaw University of Technology, 75 Koszykowa Street, 00-662 Warsaw, Poland
[2] Astronika Sp. z o.o., 18 Bartycka Street, 00-716 Warsaw, Poland
[3] ILF Consulting Engineers sp. z o.o., 12 Osmańska Street, 02-823 Warsaw, Poland

Abstract. This paper presents an approach to the construction and measurements of electrodynamic and reluctance actuators. Executive elements were used as drives in a novel concept of a magnetomotive micropump. The paper discusses various aspects concerning the designation of parameters, control system, the explanation of physical phenomena, and the optimization of the basic elements for coil units. The conducted work describes the measurement system and the analysis of the derived values. The actuators were compared and the pros/cons of building the conceptual device were highlighted. The best solution to be used in the upcoming work concerning the construction of a magnetomotive micropump was chosen based on measurements, engineering aspects, layout control, and key parameters such as the piston velocity, energy stored in capacitors, and efficiencies.

Key words: control system, micropump, electrodynamic induction, magnetic acceleration.

1. Introduction

Electromagnetic field can generate force by acting on a given magnetic body and accelerating it to a high velocity. There are two ways to achieve that. The first is based on a coil with a ferromagnetic core. While the coil is energized, a strong magnetic field is formed [1]. Then the core magnetizes itself, which in turn causes the core to move toward the center of the coil. The second way involves a conductor placed in the magnetic field. From the moment the current flows through the conductor, a force is generated, causing displacement [2]. The force generated is described as the Lorentz force [3–7]:

$$F = I \cdot l \times B, \tag{1}$$

$$F = I \cdot l \cdot B \cdot \sin\alpha \tag{2}$$

where: F is force; I is current intensity; B is magnetic flux density; l is the length of the part of the conductor in the magnetic field; α is the angle between the conductor's direction and magnetic induction B.

The phenomena described above can be successfully implemented to create a drive in a linear flow micropump for industrial applications. A huge advantage of such a solution is the elimination of friction elements, which enables the pump operations in a hazardous (explosive) environment, and an expected lower failure rate and usage concerning special applications, e.g. medical and chemical. The concept of the micropump is shown in Fig. 1.

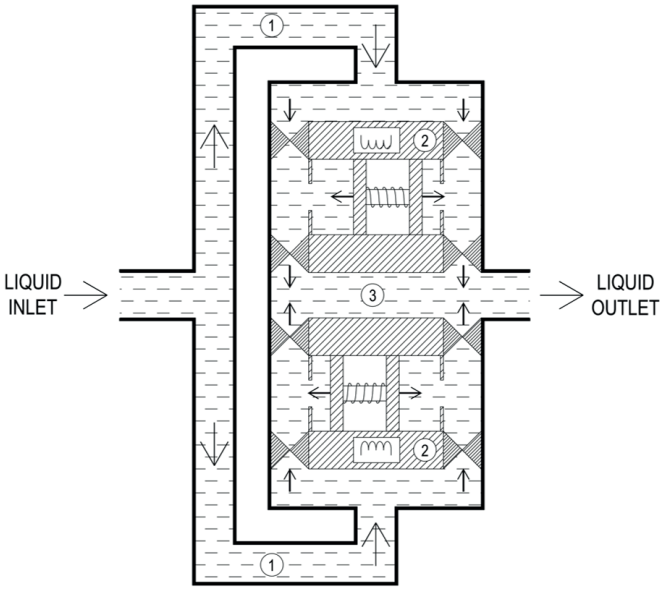

Fig. 1. The concept of the novel magnetomotive micropump: 1) inlet lines; 2) coil units; 3) collector

This micropump consists of two sections. Each section is equipped with a coil unit. The coil units are synchronized by the control system, which is discussed in this paper. The accurate control of those units is essential for guaranteeing the linear flow on the pump outlet which is directly acquired by the piston synched movement. The applied one-way valves ensure the

*e-mail: mm.szulborski@gmail.com

Manuscript submitted 2019-12-11, revised 2020-05-03, initially accepted for publication 2020-06-06, published in August 2020

medium flow in one direction. The schematic diagram of the solution is shown in Fig. 2.

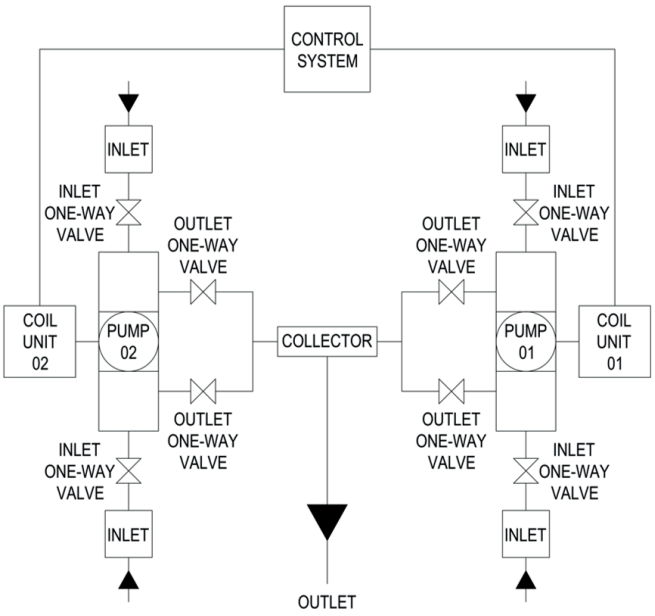

Fig. 2. The schematic diagram of the magnetomotive micropump

This paper focuses on proposing the most efficient and accurate control system for coil units being a key element of the application – magnetomotive micropump. Two variants of coil actuators were taken into consideration: a reluctance actuator and an electrodynamic actuator. The measurements of the electrical and mechanical parameters (piston velocity, energy) were made. For those two variants of the coil, actuators were considered. Moreover, the control and measurement systems were constructed and tested on a laboratory scale for two variants of actuators along with software (program code) obtained for achieving the desired functionality of the control system. The selection of the necessary components was justified and explained by the theoretical and practical calculations.

2. Review of technical solutions

Pumps are used as machines necessary for the proper functioning of industrial plants with different business profiles. Their diversity is impressive, so they are applicable in a variety of pumping installations for almost any medium. While pumping, the device receives mechanical energy from the drive motor, and then transfers it to the medium flowing through the device using a rotor, piston, shaft, etc. As a result, the energy of the medium is lifted and increases. It should be added that pumps are passive hydraulic devices since those devices draw energy from the outside. Electric motors, internal combustion engines, and steam turbines are most often used drives in such devices. Importantly, the pump drive can be controlled directly or indirectly via gears. However, the solutions used often have a significant size (even for low power devices) and no compact construction. Most of them have numerous friction elements (easily perishable). There are difficulties in expansion with an existing application and a problem with ensuring a linear flow of the medium. The authors were guided by the idea of building a pump that provides:

- increased durability (no friction elements),
- guarantee of a linear flow of the medium (not only liquids but also gases),
- full scalability in the range of active power from four to hundreds of watts,
- the opportunity to work in a specialized environment (gas, chemical),
- easy expansion – connecting pumps,
- unique way of working (the precise way of switching sections).

An analysis of the physical phenomena associated with the work of these systems was conducted in the work on the construction of the actuators for the magnetomotive micropump. This was considered in research and tests and a lot of attention was paid to the proper control of the reluctance and electrodynamic actuator piston (determining the optimal moment of switching on the next coil). Research and tests concerning the employment of the actuator were conducted to give an answer on the type and the scope of the device implementation. Studies of physical phenomena and literature concerning an electromagnetic actuator have already made it possible to optimize the parameters of the capacitance of capacitors, the number of capacitors, and the number of coils. The guidelines were as follows: possibly high kinetic energy, constant piston length, possibly low mass of the piston itself, and thus a cylinder, compact design.

Currently, presented solutions are often one-coil section structures and most likely classical electromagnet designs. Therefore, the analysis of the time and place of enclosing individual sections is unnecessary. There are constructions with high tare masses and limited operating frequency [8]. Obviously, the presented results are ordered and used by the authors to determine the direction of work. As far as calculations and methodology are concerned, a comprehensive description can be found in [9]. This paper presents the design study of a lightweight inertial actuator with an integrated velocity sensor, for the implementation of velocity feedback control, i.e. active damping, in lightly damped panels. However, in the literature, the model presented does not clearly combine analytical and numerical calculations for actuators with linear fluid flow. A transparent way of designing and testing such executive elements by building a repeatable test stand was not found. There are still constructions with high tare masses and limited operating frequency, e.g. in [10]. A half-practical solution was presented by a team of Chinese researchers [11]. The authors used several excellent studies on electromagnetic structures, where they presented methods for calculating electrical machines [12–16]. Undoubtedly, the presented model also shows how to control the flow so that it is linear, which is often key in applications in the medical and chemical industries.

3. Reluctance actuator

A reluctance actuator consists of a coil and a ferromagnetic piston. When the current passes through the coil, the force acts on the piston on its periphery. It pulls the piston inside the solenoid and tends to hold it in the middle of the coil. However, if the current is cut off at the proper moment of piston moving toward the center of the coil, the piston acquires kinetic energy. The velocity of the ferromagnetic body would be high enough to exit the coil through the other end. It does not matter on which side of the coil the body is placed. The element always attains the opposite polarity and as a result is magnetized by the energized solenoid and pulled inside the coil. In this paper certain parameters of the reluctance actuator elements were determined via proper calculations and analysis [17].

3.1. Coil geometry (length and diameter). A properly designed coil geometry can increase the efficiency of the actuator, reduce kinetic energy losses, and thus increase the velocity of the piston. To determine the maximum efficiency of the coil, the Fabry method was used with variables describing the designed solenoid geometry. Two parameters have been defined: $\alpha = \alpha_2/\alpha_1$ (α_1 is the inside coil radius; α_2 is the outside coil radius), and $\beta = b/\alpha_1$ (b is the half of the coil length). The dimensionless geometric coefficient, also known as Febry's factor, is a function of these two parameters. It is not dependent on the size of the coil but only on its shape:

$$G(\alpha,\beta) = \frac{\sqrt{2\pi}}{5} \cdot \sqrt{\frac{\beta}{\alpha^2-1}} \cdot \ln\left(\frac{\alpha+\sqrt{\alpha^2+\beta^2}}{1+\sqrt{1+\beta^2}}\right). \tag{3}$$

The value of the Febry's factor $G(\alpha,\beta)$ ranges from 0 to ~0.179. The maximum value is reached for $\alpha = 3.1$ and $\beta = 1.875$, which means that the solenoid with the shape defined by such parameters generates the highest magnetic field intensity for the given power load. The dependency describing the value of the magnetic field strength in the center of the coil, considering the Febry's factor $G(\alpha,\beta)$ is shown below [1]:

$$H_0 = \sqrt{\frac{P\cdot\lambda}{\alpha_1\cdot\rho}} \cdot G(\alpha,\beta) \tag{4}$$

where: H_0 is the intensity of the magnetic field in the center of the coil; P is power taken by the coil; λ is the space factor (for a wire with a circular cross-section $\lambda = \pi/4$); ρ is the resistivity of the winding wire.

For a constant internal diameter and an assumed power of 50 W, the coil shape was optimized for different values of the outside diameter and the length of the coil. The plane that represents maximum efficiency is shown in Fig. 3. Optimal results for the designed coil: length (L) – 1.5 cm, radius (α_2) – 2.48 cm. Values were derived for the highest magnetic field intensity value: $G(\alpha,\beta) = 0.179$.

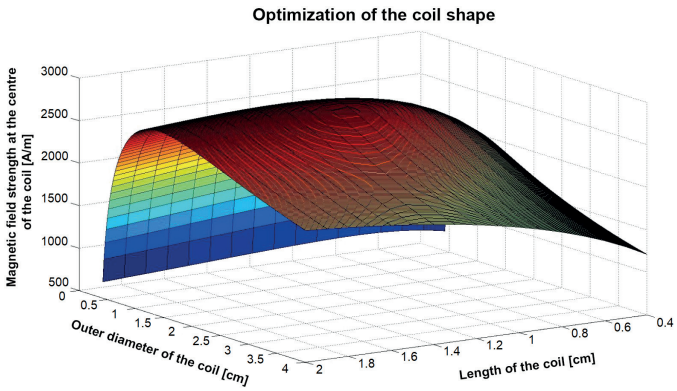

Fig. 3. The intensity of the magnetic field in the center of the coil as a function of the length and the diameter of the designed coil

3.2. Thickness of the coil winding The next parameter affecting the efficiency of the reluctance actuator is the thickness of the winding wire. The change in the wire diameter is related to the change in the number of coils and the resistance of the entire coil unit. The first step was to determine the resistance. The space factor λ, which has already been used, is the ratio of the cross-sectional area of the wire S_d to the surface area S_z that takes up one roll and is equal to $\pi/4$. Assuming that the space factor is a constant in the entire coil, the volume of the winding wire V_d is expressed in relation to the total volume V_c [18, 19]:

$$V_c = \pi\cdot\left(a_2^2 - a_1^2\right)\cdot L, \tag{5}$$

$$V_d = \lambda\cdot V_c, \tag{6}$$

$$V_d = \pi\cdot\lambda\cdot\left(a_2^2 - a_1^2\right)\cdot L. \tag{7}$$

With the total volume of the wire, its length L_d was determined by dividing the wire volume by the cross-sectional area of the coil [1]:

$$L_d = \frac{V_d}{S_d}, \tag{8}$$

$$L_d = \frac{4\cdot\lambda\cdot\left(a_2^2 - a_1^2\right)\cdot L}{\phi^2}. \tag{9}$$

Using the wire length L_d, its cross-sectional area S_d, the resistivity ρ of the material and angle ϕ for the contour curve s, the coil resistance R_c was determined:

$$R_c = \rho\cdot\frac{L_d}{S_d}, \tag{10}$$

$$R_c = \frac{16\cdot\rho\cdot\lambda\cdot\left(a_2^2 - a_1^2\right)\cdot L}{\pi\cdot\phi^4}. \tag{11}$$

The current density in the winding J is given by the equation:

$$J = \frac{I_c}{S_d}. \tag{12}$$

To obtain the current density J_c for the coil, the dependence is multiplied by the space factor λ:

$$J_c = \lambda \cdot \frac{I_c}{S_d}. \tag{13}$$

The value of the current I_c flowing in the coil depends on the resistance of the coil R_c, the external resistance R_z and voltage U (the sum of resistances of all circuit elements except for the coil).

$$I_c = \frac{U}{R_c + R_z}. \tag{14}$$

The combination of this dependency with the formula describing the resistance facilitated determining the current density in the coil:

$$J_c = \lambda \cdot \frac{U}{\frac{1}{4} \cdot \pi \cdot \phi^2 \cdot R_z + \frac{4 \cdot \lambda \cdot \rho \cdot \left(a_2^2 - a_1^2\right) \cdot L}{\phi^2}}. \tag{15}$$

The above dependencies were implemented and the J_c values were derived for several different wire diameters. The result is shown in Fig. 4. Derived calculations uncovered that the highest current density occurs in a wire with a diameter of 1.1 mm.

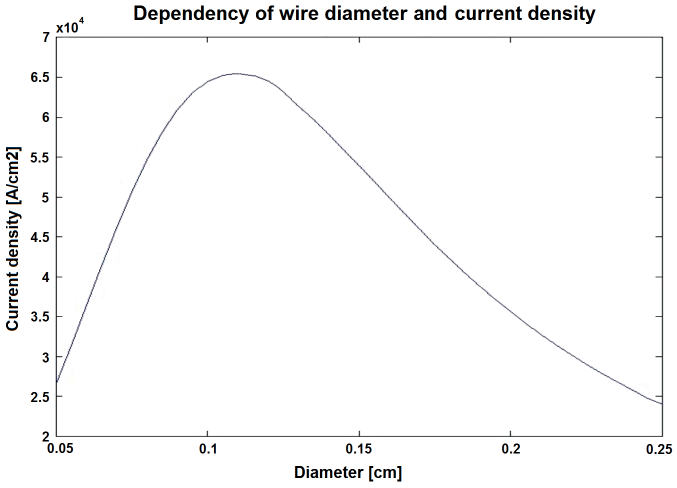

Fig. 4. Dependency between the current density and the diameter of the winding wire

3.3. Piston material. In the case of a reluctance actuator, the construction material of the piston is of high importance. The best efficiency is achieved when the core is demagnetized as fast as possible after exiting the coil. Carbon steel, which was assigned as a piston material, has the best properties in this respect. The non-linear magnetization characteristics of steel were also considered during the material selection.

4. Electrodynamic actuator

The electrodynamic actuator is also equipped with a coil and a piston. However, the piston is a non-ferromagnetic conductor – it can be a copper tube, a cylinder, or even a second coil. The piston is pushed out by the force generated as a result of the eddy currents induced in it. Currents interact with the radial component of the magnetic field, thereby causing the piston to move. However, the piston does not work with the force that causes it to accelerate only. The circuit that accelerates the piston consists of a capacitor with a capacity of C charged to a certain voltage level. The driving element is the inductance L which produces a magnetic field inducing the current in the piston. The resistance of the current in the circuit with the capacitor is affected by its resistance and the resistance of the wire from which the coil is built. The important parameter is M_{cp} – mutual inductance between the coil and the piston. The parameter determines the electrical energy conversion into the kinetic energy of the piston. The most important parameters for electrodynamic actuators were described below [20].

4.1. Voltage. The influence of voltage has been tested in the range from 0 V to 800 V, taking the 100 V step between successive values. With increasing voltage, the equivalent capacity was always equal to 250 μF. In contrast, the effect of the volume was tested in the range of 0 V to 500 μF, taking the 100 μF step between the successive values. While increasing the capacity, the voltage was equal to 700 V. The diagram is presented in Fig. 5.

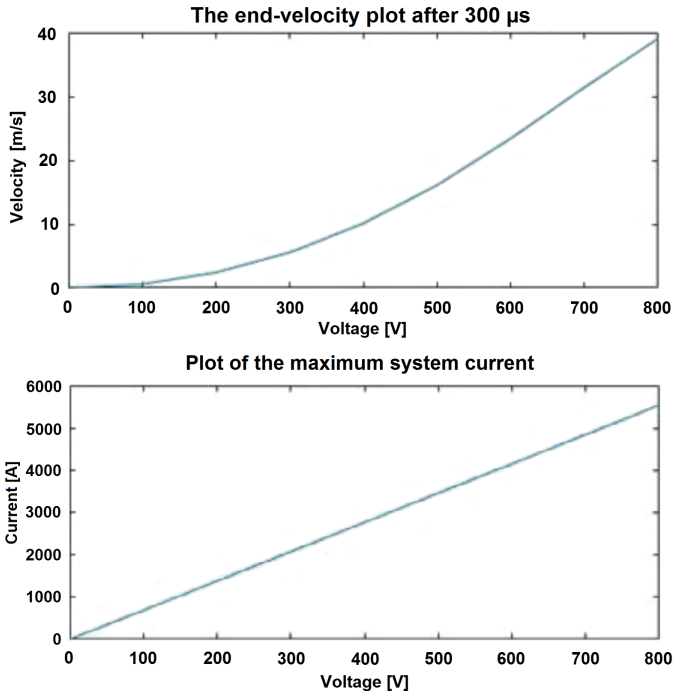

Fig. 5. Dependency between the force and the velocity over time and the capacitor voltage value for a 14-mm quadrilateral coil

The speed increased exponentially with the voltage. Electrical energy was converted into the kinetic energy of the piston.

4.2. Mutual inductance. The piston in the electrodynamic actuator is a copper tube. The tube has a lower mass compared to the full cylinder and, due to very short times of inducting the

currents, the whole phenomena is observed on the surface of the piston. Therefore, reducing the weight by using a tube does not affect the energy losses, and increases the acceleration. The external circuit was characterized by a 700 V capacitor with a capacity equal to 250 μF. The coil had an internal diameter of 8.2 mm, a length of 30 mm, and a thickness of 3 mm. The obtained graphs are presented in Fig. 6.

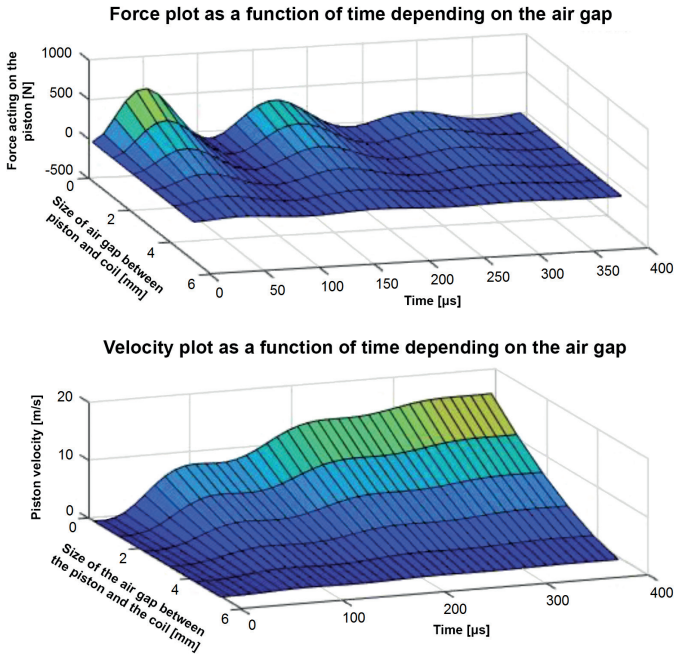

Fig. 6. Dependency between the force and the velocity over time depending on the air gap for the coil

A smaller gap causes greater magnetic coupling between the coil and the piston, which results in a better energy conversion in the system. Looking at the graphs, it is clear that reducing the gap definitely increases the force acting on the piston. The greater the force, the higher the speed of the piston, and, as a result, the greater its kinetic energy is.

4.3. Coil geometry and dimensions. To determine the optimal parameters of the coils, dependencies like those for the reluctance actuator were used, except for the formulation of Febry's factor (layer coil) [1]:

$$G = \frac{\sqrt{\pi a_1}}{5} \cdot \sqrt{\int_{a_1}^{a_2} \frac{\lambda^+}{\rho^+} \frac{z}{rs^2}\, dr} \tag{16}$$

where: dr is the cylinder thickness in cm; z is the length in cm; a_1 is the inside coil radius in cm; a_2 is the outside coil radius in cm; ρ is resistance in ohm·cm; r is the half-cylinder height in cm; s is the cylinder diagonal in cm.

Based on the previous simulations, a vast number of fixed parameters was assumed. The coil unit is set to be supplied with two capacitors of capacity 250 μF connected in a series and charged to 700 V. The piston is determined as a 1 mm thick copper tube, 20 mm long, with the weight of 2.00 g and an external diameter of 8 mm. The coil will be wound up from a wire with a cross-section of 2 mm × 1 mm.

5. Actuators setup

During the work concerning the construction of the coil actuators for the magnetomotive micropump, an analysis of the physical phenomena associated with the optimization of these systems was conducted. Research has clearly indicated that in the reluctance actuator, due to the disappearance of the current in the preceding coil, the piston can decelerate. This occurrence had direct impact on the overall piston velocity. With the electrodynamic actuator, electromagnetic and physical mechanics tended to push the piston without deceleration. Moreover, it was assumed that the electrodynamic actuator piston will eventually have a higher kinetic energy. It was decided to construct a reluctance actuator consisting of three coil sections, while the electrodynamic actuator consisted of only two coil sections. Another feature that should be emphasized is the weight of the piston. The reluctance actuator piston was a ferromagnetic core. The weight of the piston was slightly higher than in the electrodynamic actuator (2.00 g) and was equal to 3.33 g. In our research and trials, a lot of attention was paid to the proper control of the reluctance actuator piston (determination of the optimal moment of switching on the next coil section). This did not change the fact that larger capacitance of the capacitor than for the electrodynamic actuator was used. Naturally, this resulted in an increase in the input energy of the system. Research data and attempts to use such an actuator setup were to give an answer concerning the type and scope of use in the final design of the magnetomotive micropump.

The study of the physical phenomena and literature regarding an electrodynamic actuator already facilitated lowering such parameters as the capacity of the capacitors, their quantity, and the number of coil sections.

5.1. Reluctance actuator. The heart of the control system was an 8-bit microprocessor from the AVR family – Atmega32A, clocked at 16 MHz, the microcontroller with enough digital inputs and outputs required for this project and the SPI interface allowing programming without urge to physically remove the component from the fixed system. The whole system was powered by 230 V AC mains voltage, the blue electroluminescent diode signaled the power switching status. The first stage implemented by the controller was the charging process of the capacitors. 230 V AC/110 V AC transformer and small rectifying bridges DF08 were used. Connecting and disconnecting the charging circuits of subsequent sections were conducted by PE014005 relays. The microcontroller controlled their coils through the BC547 NPN transistors, which were protected against overvoltage by the UF4007 extinguishing diodes. Capacitors were charged by 100 Ω resistors of power rating equal to 220 W. This solution reduced the charging current, which extended the life of the capacitors and made it easier to control the circuit. In parallel with capacitors: 2780 μF, 1805 μF and 860 μF, low impedance capacitors (Low ESR)

330 μF/500 V, 290 mΩ/100 Hz were used. Elements designed for high-frequency operation were not damaged by fast charging and discharging thanks to the presented solution. Such a solution would make standard impedance capacitors less vulnerable to damage resulting from the high discharge current pulse after the coil circuits were turned on. IGBT transistors were chosen as executive control elements for each coil section since they are more resistant to surge currents. Moreover, the voltage drops across the connector did not grow with the current in those transistors. After controlling the input, the voltage U = 15 V will be given to the gate of the IGBT transistor connected in a low-side configuration. The coil sections, connected on one side to the high capacitor bank capacitance, were shorted to the zero potential on the second end. The current pulse generated an electromagnetic field that set the piston in motion. Synchronization of the coils was set in such a way that the capacitors were discharged at the right time – so that the piston did not slow down after crossing the center of the coil (or slowed marginally). The described actuator and its control system were shown in Fig. 7.

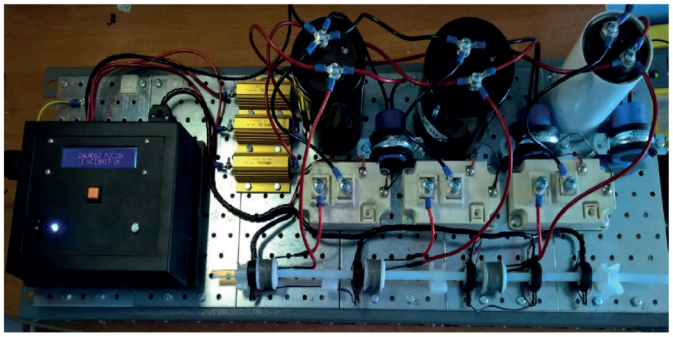

Fig. 7. Reluctance actuator and its control system

Three subsequent coil sections were controlled in the described way. Phototransistors for velocity measurement were placed on the third section at a distance of 50 mm from each other. A dedicated circuit board was created for this system to assure the best control of the described elements. A circuit board was designed considering the appropriate housing, from which four connectors, the LCD display and the LED diode would be outputted and a button initiating the successive stages of the program would be executed. Connectors would connect in sequence: IEC 320 C14 – 230 V AC power supply, DB15 – IR luminescent diodes, phototransistors and IGBT gate control signals, Molex 4P – charged of three capacitor banks, IDC 10P – ISP/KANDA standard programmer.

5.2. Electrodynamic actuator. The FR5739 microcontroller from Texas Instruments, a member of the MSP430 family, was selected for the role of the main control system component. Microcontrollers from this family were compatible with the von Neumann architecture, whose most important feature is energy efficiency. In addition, the microcontroller is equipped with FRAM memory (Ferroelectric Random Access Memory), which was characterized by high data writing speed. The clock frequency of 24 MHz was sufficient for the system. Due to the different supply voltages of components included in the control and measurement system, it was necessary to use voltage stabilizers to obtain a voltage of 3.3 V and 5 V. Stabilizers LM78xx were chosen. To realize the measurement of the piston velocity in the solenoid, photodiode BPW34 was chosen. These photodiodes react to light waves in a wide spectral range. Photodiodes were placed on the second section at a distance of 50 mm from each other. Essential elements in the system were also capacitors that filter signals and provide a reserve of energy at a sudden demand. Each section consisted of two capacitors with a value of 125 μF (single capacitor) and a voltage equal to 400 V. The controller also used resistors, ARK-2 connectors, a mini USB connector, a gold pin connector and signaling diodes as well as switches that enabled interaction. To charge the capacitors, miniature JQX-115F ZS3 power relays were used. The moment the high state appeared on the appropriate pin of the microcontroller, the coil was connected by 12 V pin with the LTV816 optocoupler. The coil attracted a contact that allowed the capacitor to be charged. When the desired voltage was reached on the capacitor, the signal on the microcontroller output changed to low and the coil was disconnected. Power supply was IEC 320 C14 – 230 V AC, as in the case of a reluctance actuator.

Moreover, as for a reluctance actuator, the custom circuit board was designed to control the described elements. The model of the electromagnetic actuator with control and measurement system are shown in Fig. 8. A schematic diagram of the control system is presented in Fig. 9.

(a)

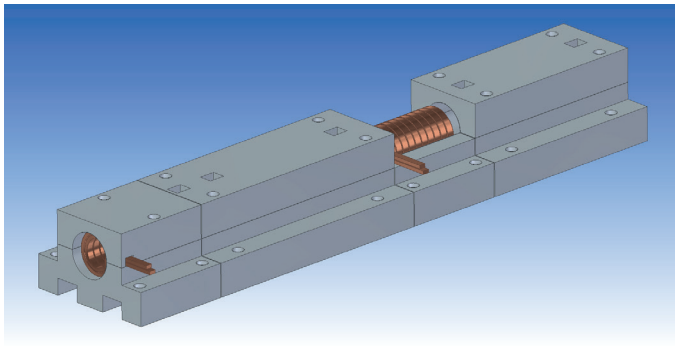

(b)

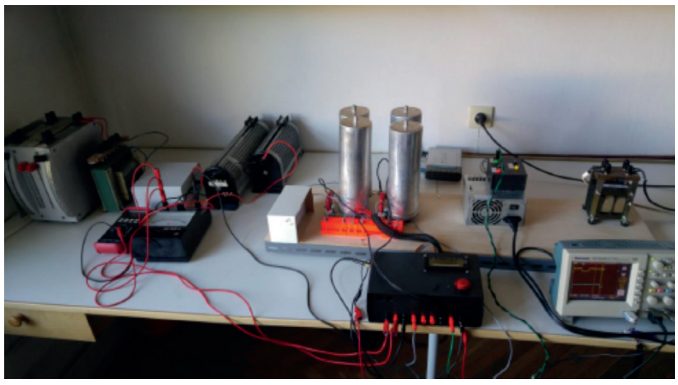

Fig. 8. Electrodynamic actuator and its control system: a) fragment of the electrodynamic actuator chassis; b) laboratory setup

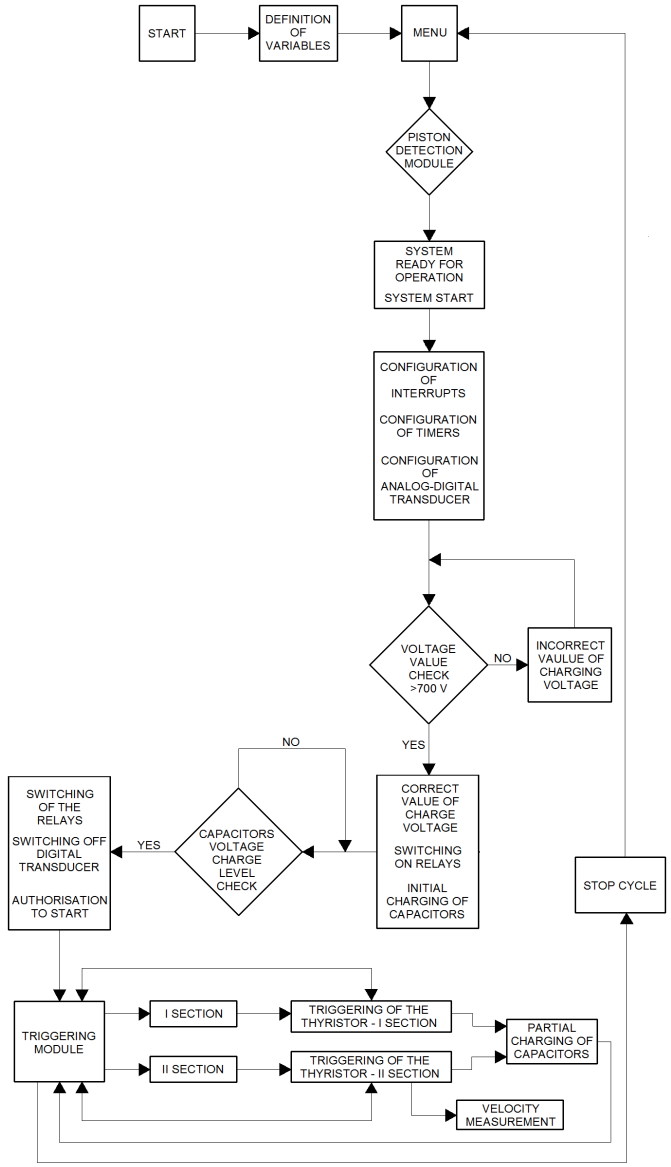

Fig. 9. Reluctance actuator and its control system

Table 1
Reluctance actuator – results of measurements

Actuator type	Reluctance actuator				
Description	Velocity measurements results after III coil section				
Series number	1	2	3	4	5
Time [ms]	1.323	1.339	1.336	1.335	1.335
Velocity [m/s]	37.326	37.530	37.425	37.439	37.453
Velocity average value [m/s]	37.435				
Average kinetic energy accumulated in capacitors [J]	77.312				
Average kinetic energy of the piston [J]	2.344				
Efficiency [%]	3.030				

Table 2
Electrodynamic actuator – results of measurements

Actuator type	Reluctance actuator				
Description	Velocity measurements results after II coil section				
Series number	1	2	3	4	5
Time [ms]	1.600	1.450	1.500	1.450	1.465
Velocity [m/s]	31.250	34.480	33.330	34.480	34.12
Velocity average value [m/s]	33.532				
Average kinetic energy accumulated in capacitors [J]	40.000				
Average kinetic energy of the piston [J]	1.124				
Efficiency [%]	2.810				

6. Measurements results

A series of measurements was arranged to determine the piston velocity after III coil section for the reluctance actuator and II coil section for the electrodynamic actuator. The five-measurement series for each actuator type was conducted. The results were presented in Table 1 and Table 2.

Oscillograph records taken from the detectors measuring the range for the reluctance actuator after III coil section and for the electrodynamic actuator after II coil section were presented in Figs. 10 and 11.

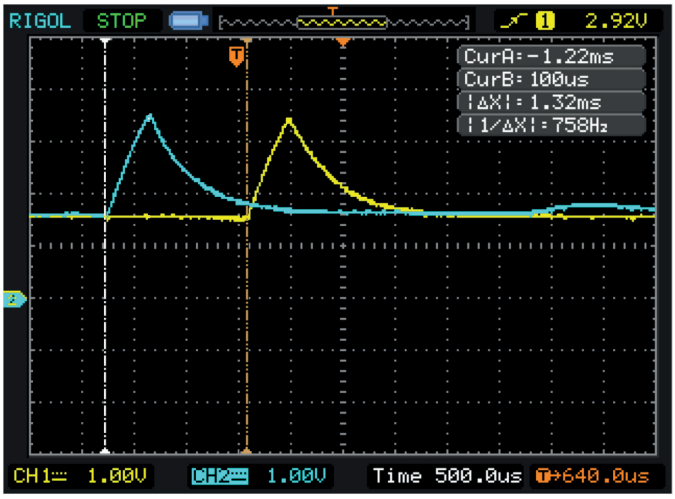

Fig. 10. ROscillograph record determining the piston velocity after the third section of the reluctance actuator. Detector: phototransistors

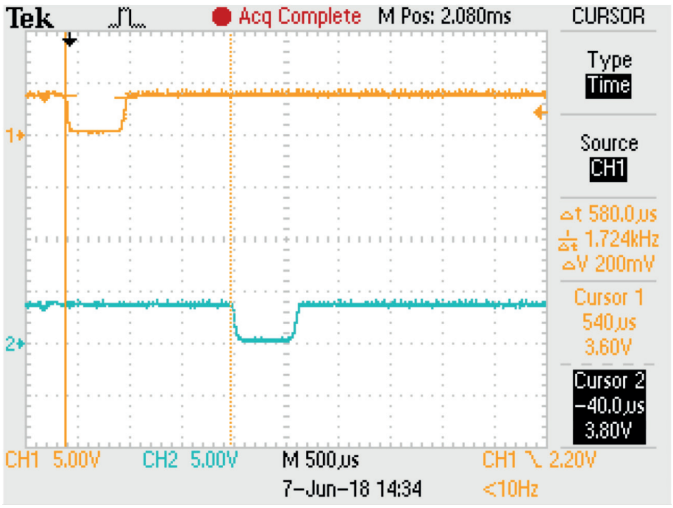

Fig. 11. ROscillograph record determining the piston velocity after the second section of the electrodynamic actuator. Detector: photodiodes

7. Discussion about measurements

The efficiencies of both actuators are acceptable during the prototype stage, as presented in Tables 1 and 2. Undoubtedly, attention should be paid to the mechanics of these devices. The coil units should be fast and precise – it was decided to use elements executive with pulse power supply. In electromagnetic micromachinery constructions developed worldwide, employing the aforementioned type of power supply, the expected efficiency is around 5%. Larger electromagnetic devices with pulse power supply reach 11% [21, 22]. The electrodynamic actuator reached an efficiency of 2.8%, while the reluctance actuator reached an efficiency of 3.0%. The constructed electrodynamic actuator consisted of two coil sections. The efficiencies were in the same range despite the fact the electrodynamic actuator piston is much lighter, and the entire construction is favorable in terms of quality, durability, versatility, and the best performance. The abovementioned depend strictly on the materials that were used to design and shape the element chassis and piston. The shape of the mentioned element is ideal for implementation. Moreover, smaller capacity and voltage are involved, which is also favorable. On the other hand, the reluctance actuator consisting of three coil sections is much heavier as the control system is also more complex, considering the control of residual stream caused by the current shift. That may lead to issues during the implementation.

Measuring systems employing different types of detectors were proposed to conduct measurements. The peak characteristic witnessed on the oscillograph record presented in Fig. 10 is the effect of piston partially covering the detector while moving towards it. The peak characteristic is standard for a phototransistor. The photodiodes that were used as detectors in the case of the electrodynamic actuator exhibit a wider peak than those observed in the series involving a phototransistor (Fig. 11). Measurement ranges were marked on the oscillograph records to present the variation of time values obtained during the measurements. The differences in the measured velocity values in the series can be associated with the factors that were not included in the simulations and laboratory work at the prototype stage, including friction and drag, initial piston position error, and also the difference and magnetization curve of the actual material. This means that the greatest losses occur while converting the electrical force into a magnetomotive force that sets the piston in motion.

Table 3
Electrodynamic actuator – results of measurements

Actuator type	Reluctance actuator		Electrodynamic actuator	
Description	Velocity measurement summary		Velocity measurement summary	
Method	Laboratory	FEM	Laboratory	FEM
Velocity [m/s]	37.530	42.120	34.480	39.47
Velocity difference [m/s]	4.59		4.99	
Average kinetic energy of the piston difference [J]	0.369		0.389	
Efficiency difference [%]	0.84		0.92	

Simulations employing the Finite Element Method were conducted to create reference results for both coil units. The summary of the laboratory results and simulation results is presented in Table 3. The FEM simulations represent ideal conditions. Therefore, the results are slightly better. However, the derived values still fall within the range of those obtained from the laboratory work.

8. Conclusions

The team of authors examined two types of actuators in terms of usage, by means of constructing the electromagnetic micropump. The subjects of the research presented in this paper were coil units in both reluctance and electrodynamic versions. Two actuators involving different control systems were designed, constructed, and compared. The results of the comparison are as follows:

- The electrodynamic actuator is more compact.
- The electrodynamic actuator exhibits better efficiency in comparison to the reluctance actuator.
- The control system for the electrodynamic actuator is easier to implement.
- The estimated length of service for the electrodynamic actuator is estimated as longer in comparison to the reluctance actuator (the control system, the complexity of the solution).
- The reluctance actuator requires a bigger and heavier chassis construction.
- The piston is heavier in the prototype of the reluctance actuator.

- A compensating residual stream caused by the current shift causes difficulties related to the reluctance actuator control system.

Finally, it was settled that the electrodynamic actuator will be implemented into the novel concept of a magnetomotive micropump. Some construction aspects may change during the intended and upcoming assignments concerning the described scientific and engineering work, for example, the dimensions of the basic elements that will be used for the actuator assembly.

The efficiency of the solution was shown by measuring the kinetic energy of the piston and the efficiency of the system. Naturally, the selection is made only by comparing the cylinders tested.

The added value of the work is the clearly presented model of conduct while selecting the actuators for the presented pump design. Optimization of place and time of switching on the individual coil sections of the actuator was tested and presented. Instrumentation was comprehensively presented so that the tests can be repeated as a transparent procedure. The best executive element for the structure was determined.

References

[1] W.F. Gauster, "Somerbasic concepts for magnet coil design", *Conference paper*, Illionois, pp. 1–17, 1959.

[2] J. Liu and T. Koseki, "3 degrees of freedom control of semi-zero-power magnetic levitation suitable for two-dimensional linear motor", *Proceedings of the Fifth International Conference on Electrical Machines and Systems*, Shenyang, China, pp. 976 – 981, 2001.

[3] Y. An, G. Liu, P. Wang, H. Wen, and Z. Meng, "Magnetic force analysis and experiment of novel permanent magnet axial thrust balance structure in canned motor pump", *IEEE 2nd International Conference on Advanced Computer Control*, Shenyang, China, vol. 1, pp. 1–8, 2010.

[4] J. Cai and Y. Deng, "Initial Rotor Position Estimation and Sensorless Control of SRM Based on Coordinate Transformation", *IEEE Trans. Instrum. Meas*. 64 (4), 1004–1018 (2015).

[5] A. Masi, A. Danisi, R. Losito, and R. Perriard, "Characterization of magnetic immunity of an ironless inductive position sensor", *IEEE Sens. J*. 13 (3), 941–948 (2013).

[6] K. Yongdae, H.Y. Choi, and Y.CH. Lee, "Design and preliminary evaluation of high-temperature position sensors for aerospace applications", *IEEE Sens. J*. 14 (11), 4018–4025 (2014).

[7] F. Khoshnoud, and C.W. Silva, "Recent advances in MEMS sensor technology-mechanical applications", *IEEE Trans. Instrum. Meas*. 15 (2), 14–24 (2012).

[8] G. Loussert, "An Efficient and Optimal Moving Magnet Actuator for Active Vibration Control", *15 th International Conference on New Actuators*, Bremen, Germany, pp. 1390–1420, 2016.

[9] C. Paulitsch, P. Gardonio, S.J. Elliott, P. Sas, and R. Boonen, "Design of a Lightweight, Electrodynamic, Inertial Actuator with Integrated Velocity Sensor for Active Vibration Control of a Thin Lightly-Damped Panel", *Proceedings of ISMA*, pp. 239–251, 2004.

[10] C. Paulitsch, P. Gardonio, and S.J. Elliott, "Active vibration damping using an interial, electrodynamic actuator", *J. Vib. Acoust.* 129, 39-47 (2007).

[11] X. Li, K. Tian, and Y. Zhou, "Linear Electromagnetic Oil Pumping Unit Based on the Principle of Coil Gun", *IEEE Conference*, China, 2008.

[12] P. Fang, F. Ding, and Q. Li, "Novel High-Response Electromagnetic Actuator for Electronic Engraving System", *IEEE Trans. Magn.* 42 (3), 460–464 (2006).

[13] Y. Nakanishi, T. Honda, K. Kasamura, Y. Nakashima, K. Nakano, K. Kondo, and H. Higaki, "Bio-inspired shaft seal in coolant pump for electric vehicles", *IEEE International Conference on Renewable Energy Research and Applications (ICRERA)*, 2016.

[14] R.E. Clark, G.W. Jewell, S.J. Forrest, J. Rens, and J. Maerky, "Design Features for Enhancing the Performance of Electromagnetic Valve Actuation Systems", *IEEE Trans. Magn.* 41 (3), 692–696 (2005).

[15] H. Hoshi, T. Shinshi, and S. Takatani, "Third-generation blood pumps with mechanical noncontact magnetic bearings", *Artif. Organs* 30 (5), 324–338 (2006).

[16] J.F. Antaki, B. Paden, G. Burgreen, and N.J. Groom, "Blood pump having a magnetically suspended rotor", US Patent, No: 6447266 B2, 2002.

[17] J. Albert, R. Banucu, W. Hafla, and W.M. Rucker, "Simulation based development of a valve actuator for alternative drives using BEM-FEM code", *IEEE Trans. Magn*. 45 (3), 1744–1747 (2009).

[18] M.P. Goldowsky, "Magnetic suspension blood pump", US Patent, No: 6527699 B1, 2003.

[19] D. Elata, "On the static and dynamic response of electrostatic actuators", *Bull. Pol. Ac.: Tech*. 53 (4), 373–384 (2005).

[20] S.M. Yang and M.S. Huang, "Design and Implementation of a Magnetically Levitated Single- Axis Controlled Axial Blood Pump", *IEEE Trans. Ind. Electron*. 56 (6), 2213–2219 (2009).

[21] M.B. Khamesee and E. Shameli, "Pole piece effect on improvement of magnetic controllability for noncontact micromanipulation", *IEEE Trans. Magn*. 43 (2), 533–542 (2007).

[22] B. Ozdalyan and O. Dogan, "Effect of a semi electro-mechanical engine valve on performance and emissions in a single cylinder spark ignited engine", *J. Zhejiang Univ., Sci. A*. 11 (2), 106–114 (2010).